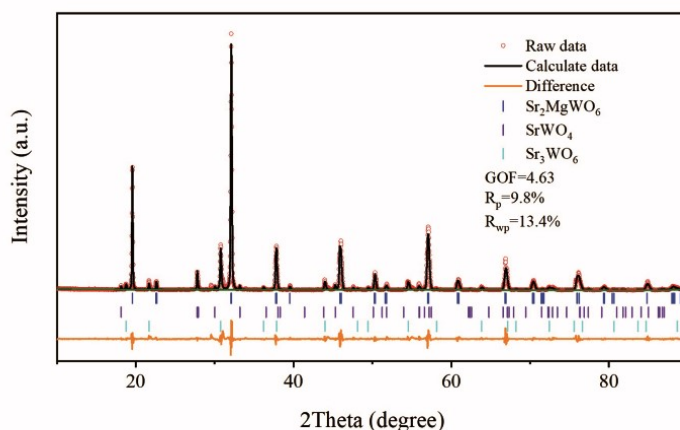


Effect of Sr²⁺ ions on the structure, upconversion emission and thermal sensing of Er³⁺, Yb³⁺ codoped double perovskites Ba_(2-x)Sr_xMgWO₆ phosphors

Guoyi Dong¹, Kexin Zhang¹, Mengrui Dong¹, Xiangxiang Li¹, Zhenyang Liu¹,
Lei Zhang^{2*}, Nian Fu^{1*}, Li Guan, Xu Li¹, Fenghe Wang^{1*}

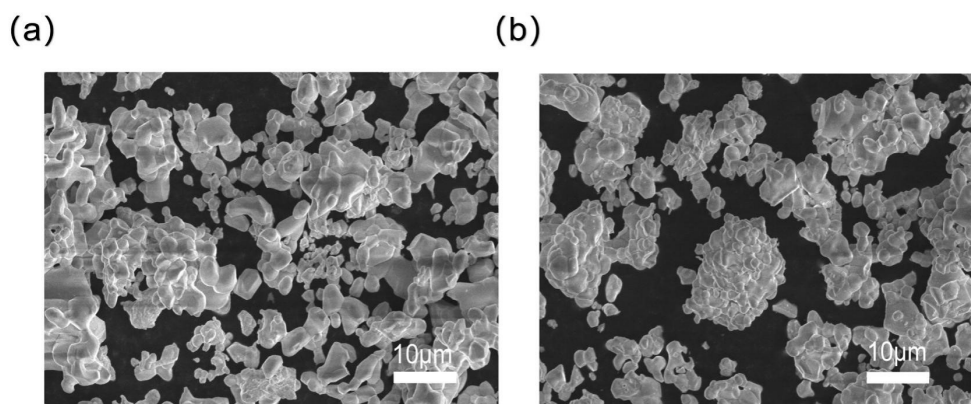
¹ Hebei Key Laboratory of Photo-Electricity Information and Materials, College of Physics Science and Technology, Hebei University, Baoding 071002, PR China

² Hebei Key Laboratory of Optoelectronic Information and Geo-detection Technology, Hebei GEO University, Shijiazhuang, China 050031

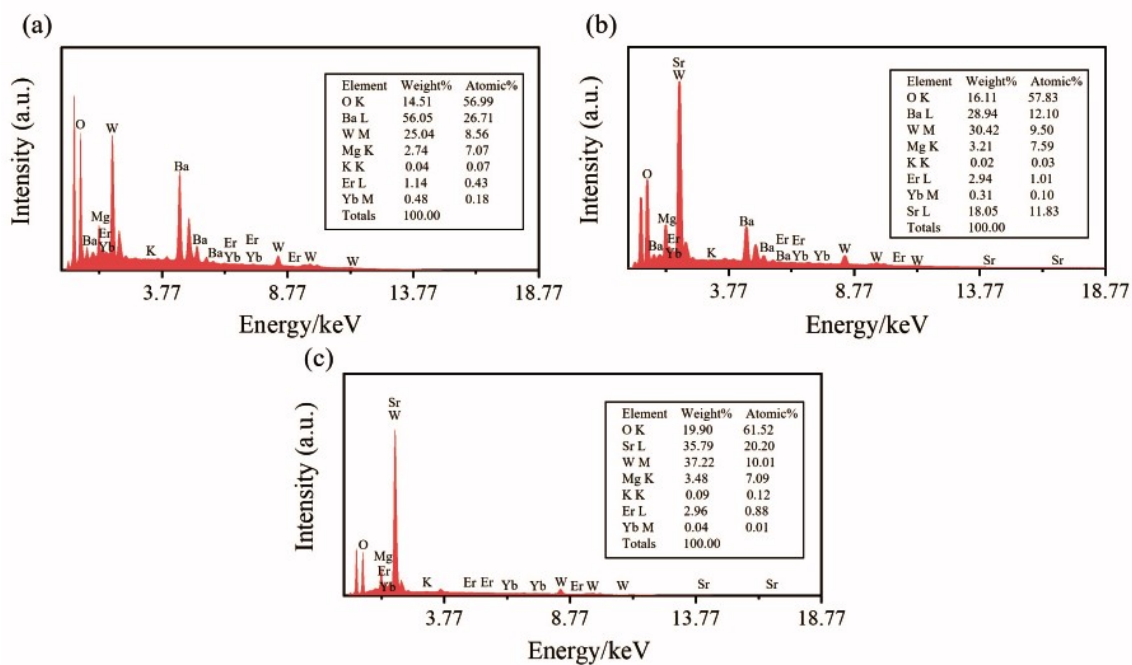


Supplementary Fig. S1. Rietveld refined XRD pattern of the Sr₂MgWO₆:7%Er³⁺, 2%Yb³⁺, 9%K⁺

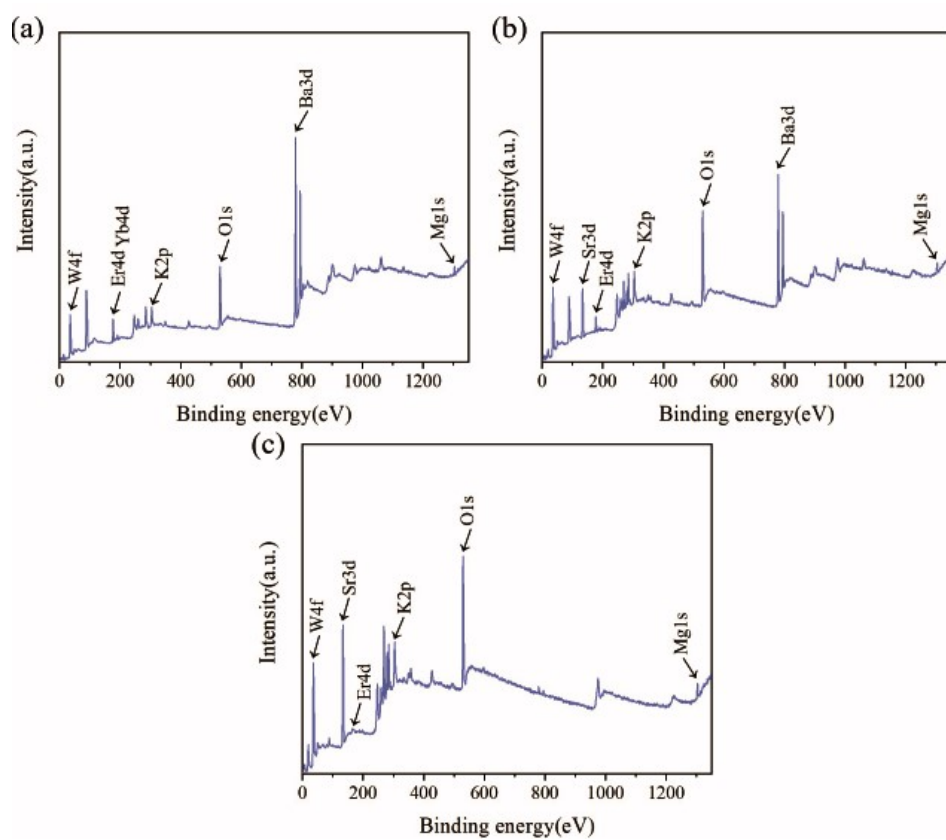
* Corresponding author: funian@hbu.edu.cn (N. Fu); zzll1012@163.com (L. Zhang); fenghe_wang@hotmail.com (F. H. Wang)



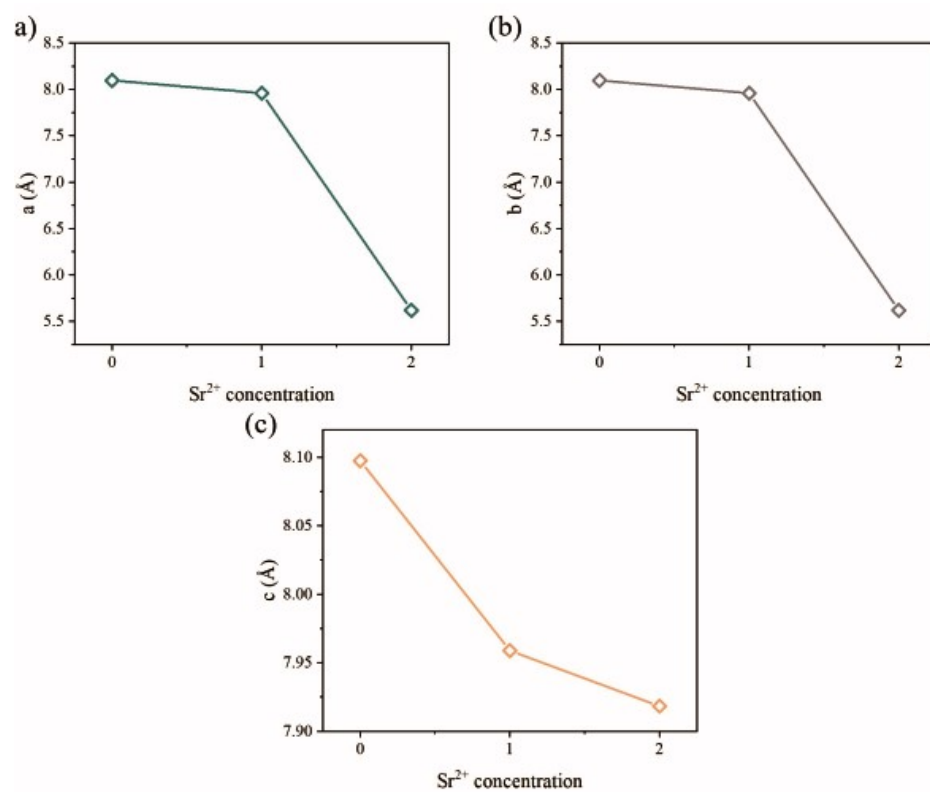
Supplementary Fig. S2. SEM images of (a) $\text{Ba}_2\text{MgWO}_6:7\%\text{Er}^{3+}, 2\%\text{Yb}^{3+}, 9\%\text{K}^+$ and (b) $\text{Sr}_2\text{MgWO}_6:7\%\text{Er}^{3+}, 2\%\text{Yb}^{3+}, 9\%\text{K}^+$



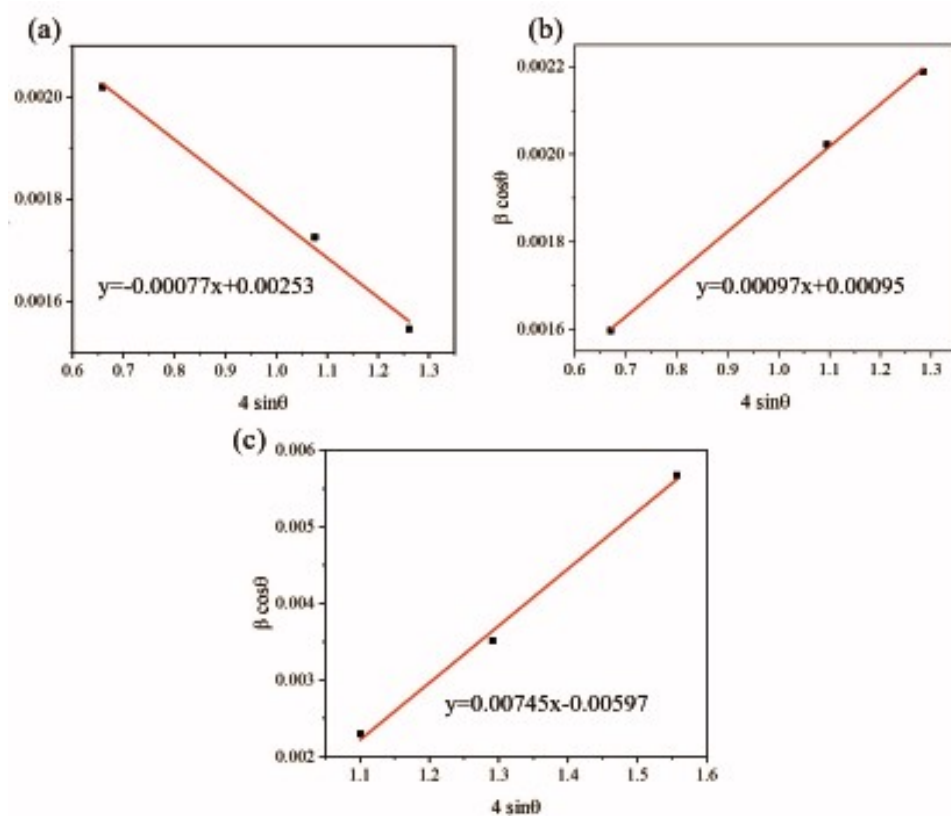
Supplementary Fig. S3. (a-c) EDS of the $\text{Ba}_{2-x}\text{Sr}_x\text{MgWO}_6:7\%\text{Er}^{3+}, 2\%\text{Yb}^{3+}, 9\%\text{K}^+$ ($x=0,1,2$)



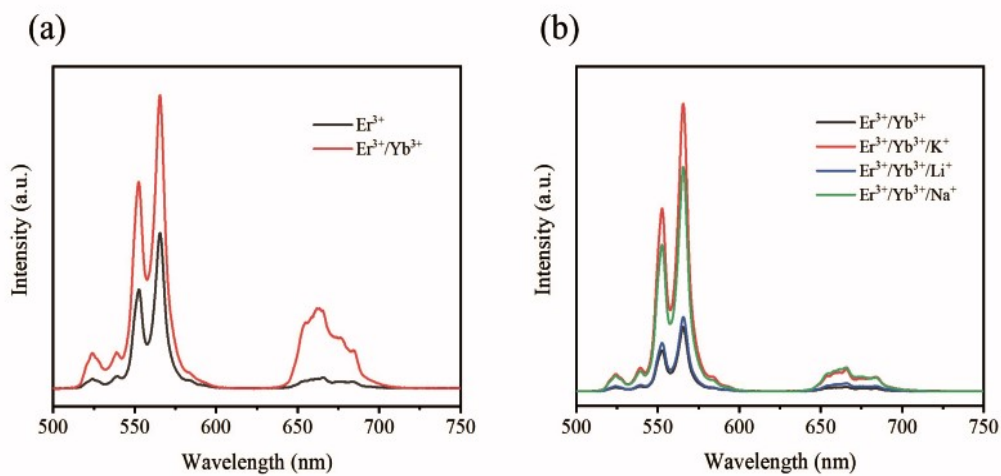
Supplementary Fig. S4. (a-c) XPS spectra of $\text{Ba}_{2-x}\text{Sr}_x\text{MgWO}_6:7\%\text{Er}^{3+}, 2\%\text{Yb}^{3+}, 9\%\text{K}^+$ ($x=0,1,2$)



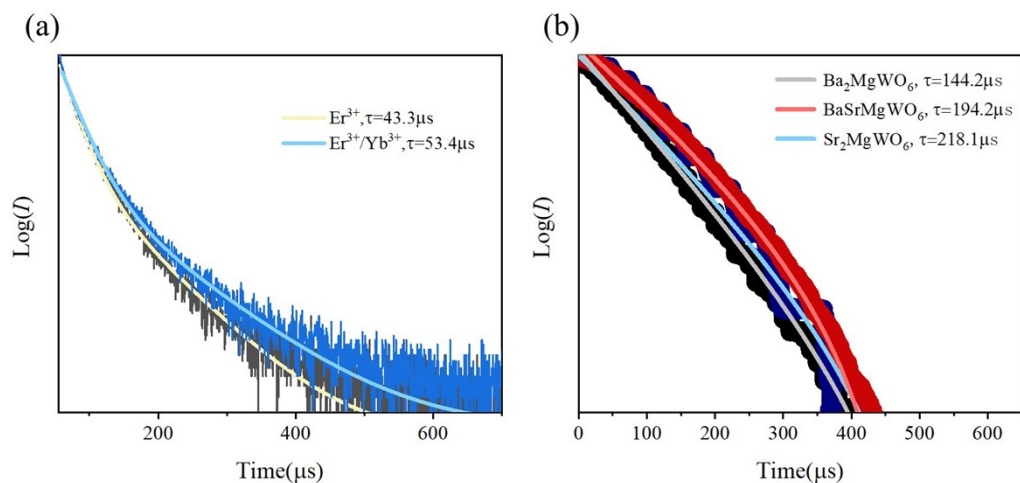
Supplementary Fig. S5. (a-c) Effect of changing Sr²⁺ doping concentration on cell parameters



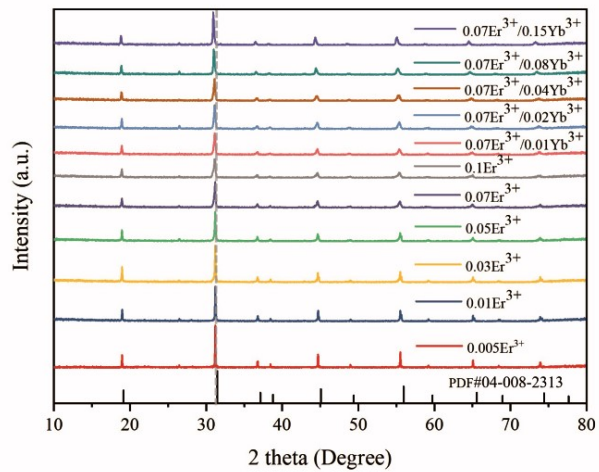
Supplementary Fig. S6. (a-c) Williamson-Hall plot of $\text{Ba}_{2-x}\text{Sr}_x\text{MgWO}_6:7\%\text{Er}^{3+}, 2\%\text{Yb}^{3+}, 9\%\text{K}^+$ ($x=0,1,2$)



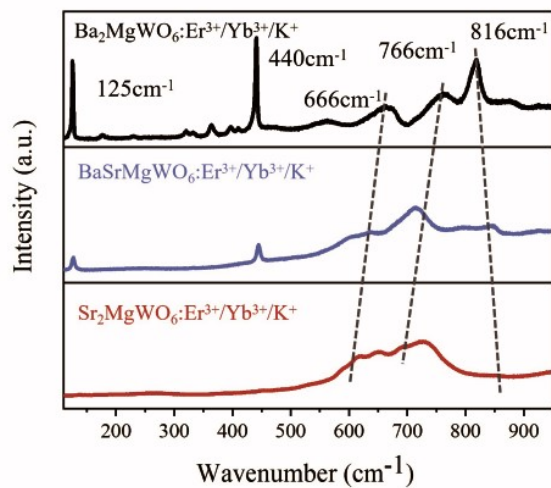
Supplementary Fig. S7. Upconversion emission spectra of (a) $\text{Sr}_2\text{Mg}_{0.93}\text{WO}_6:7\%\text{Er}^{3+}$, $\text{Sr}_2\text{Mg}_{0.91}\text{WO}_6:7\%\text{Er}^{3+}$, 2% Yb^{3+} ; (b) $\text{Sr}_2\text{Mg}_{0.91}\text{WO}_6:7\%\text{Er}^{3+}$, 2% Yb^{3+} , $\text{Sr}_2\text{Mg}_{0.91}\text{WO}_6:7\%\text{Er}^{3+}$, 2% Yb^{3+} , 9% A^+ ($\text{A} = \text{K}^+, \text{Li}^+, \text{Na}^+$)



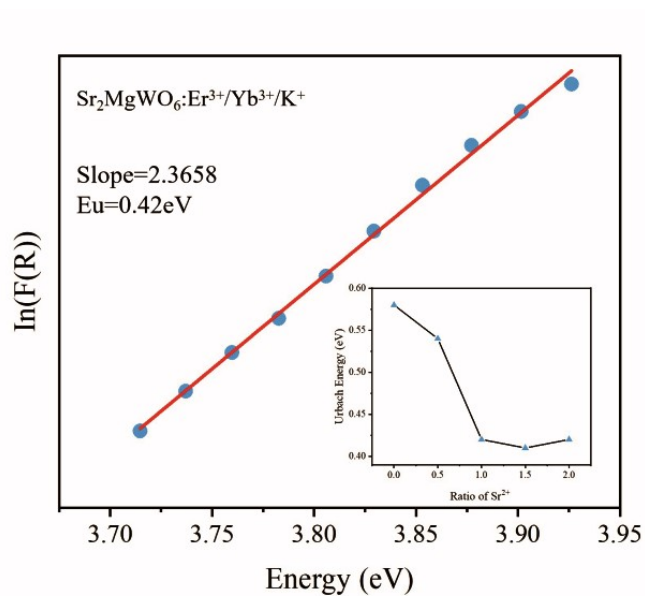
Supplementary Fig. S8. Luminescence decay curves of (a) $\text{Sr}_2\text{Mg}_{0.93}\text{WO}_6:7\%\text{Er}^{3+}$, $\text{Sr}_2\text{Mg}_{0.91}\text{WO}_6:7\%\text{Er}^{3+}$, 2% Yb^{3+} (b) $\text{Ba}_{(2-x)}\text{Sr}_x\text{MgWO}_6$ ($x=0, 1, 2$):7% Er^{3+} , 2% Yb^{3+} , 9% K^+



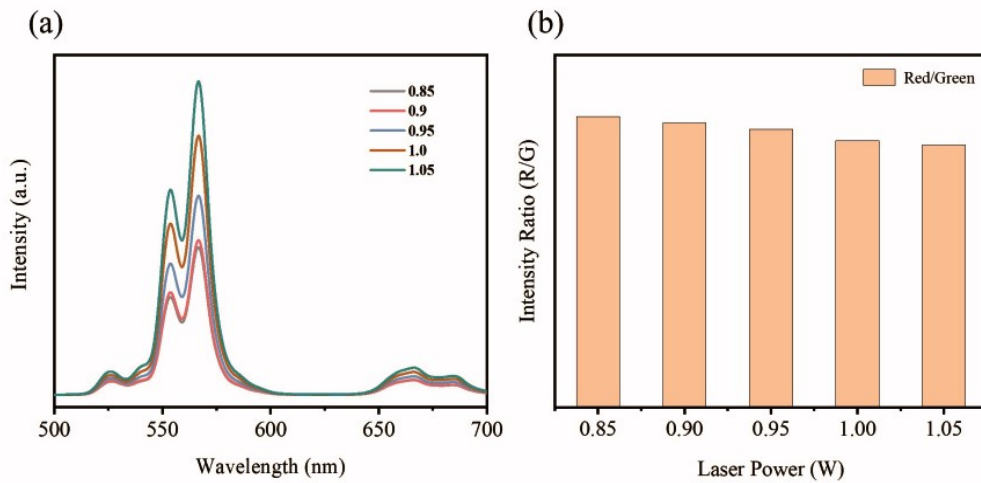
Supplementary Fig. S9. XRD sample of $\text{Sr}_2\text{Mg}_{1-m}\text{WO}_6: m\%\text{Er}^{3+}; \text{Sr}_2\text{Mg}_{0.93-n}\text{WO}_6: 7\%\text{Er}^{3+}/n\%\text{Yb}^{3+}$ ($m = 0.05, 1, 3, 5, 7, 10/n = 1, 2, 4, 8, 15$)



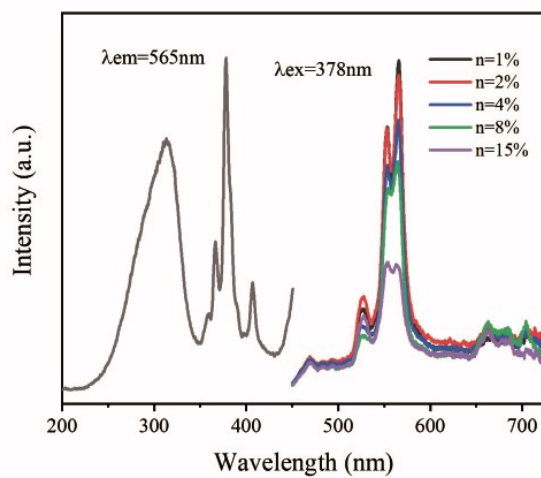
Supplementary Fig. S10. Raman spectra of $\text{Ba}_{2-x}\text{Sr}_x\text{MgWO}_6:7\%\text{Er}^{3+}, 2\%\text{Yb}^{3+}, 9\%\text{K}^+$ ($x=0, 1, 2$)



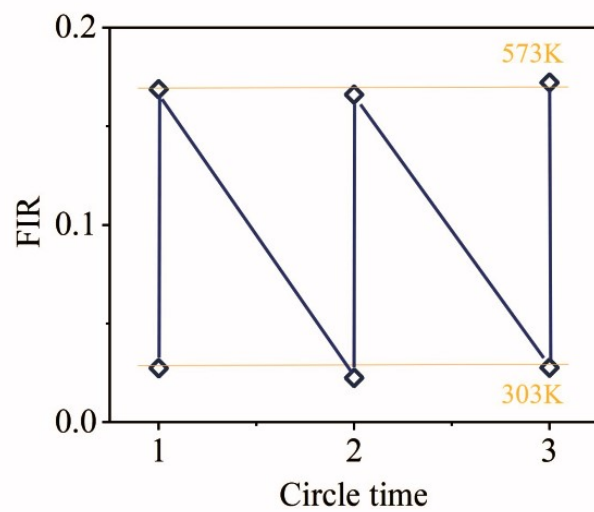
Supplementary Fig. S11. Kubelka-Munk plot $\ln(F(R))$ vs. energy plot of $\text{Sr}_2\text{MgWO}_6:7\%\text{Er}^{3+}, 2\%\text{Yb}^{3+}, 9\%\text{K}^+$, Inset shows urbach energy plot of $\text{Ba}_{2-x}\text{Sr}_x\text{MgWO}_6:7\%\text{Er}^{3+}, 2\%\text{Yb}^{3+}, 9\%\text{K}^+$ ($x=0, 0.5, 1, 1.5, 2$)



Supplementary Fig. S12. (a) Power-dependent spectra of $\text{Sr}_2\text{MgWO}_6:7\%\text{Er}^{3+}$, $2\%\text{Yb}^{3+}$, $9\%\text{K}^+$, (b) Red to green ratio of $\text{Sr}_2\text{MgWO}_6:7\%\text{Er}^{3+}$, $2\%\text{Yb}^{3+}$, $9\%\text{K}^+$ emission peak with laser power



Supplementary Fig. S13. PLE spectrum ($\lambda_{\text{em}} = 565\text{ nm}$) of $7\text{ mol}\%\text{Er}^{3+}$, $2\text{ mol}\%\text{Yb}^{3+}$: Sr_2MgWO_6 and PL spectra ($\lambda_{\text{ex}} = 378\text{ nm}$) of $2\text{ mol}\%\text{Er}^{3+}$, $n\text{ mol}\%\text{Yb}^{3+}$: Sr_2MgWO_6 ($n = 1, 2, 4, 8, 15$).



Supplementary Fig. S14. Changes in FIR (I527 nm/I553 nm) values for repeated tests between 303 K and 573 K